Characteristic Mode Analysis for Microstrip Fed Conformal Metasurface Multiband Antenna

Kothakonda Durga Bhavani[1], Boddapati T. P. Madhav[1, *], Yalavarthi Usha Devi[1],
Yarlagadda Ramakrishna[2], and Mudunuri Padmanabha Raju[3]

[1] *Antennas and Liquid Crystals Research Center, Department of ECE, Koneru Lakshmaiah Education Foundation, AP, India*
[2] *Seshadri Rao Gudlavalleru Engineering College, Gudlavalleru, AP, India*
[3] *Department of ECE, Shri Vishnu Engineering College for Women, Bhimavaram, AP, India*

ABSTRACT: In this study, an optimal multi-band microstrip fed metasurface antenna is designed. Three by three nonuniform circular radiating cross slotted elements make up the antenna's metasurface. The metasurface is analyzed using characteristic mode analysis (CMA), and the Modal Significance (MS), Characteristic angle (CA), and Eigen Value (EV) curves are utilized to optimize the antenna's performance. In addition, surface currents are examined for the metasurface and patch using CMA, and the design incorporates microstrip feeding to excite the targeted frequency bands. With its resonance frequencies of 5.4 GHz, 8.9 GHz, 12.8 GHz, 15.9 GHz, and 19.8–31.58 GHz, the developed antenna has potential uses in 5G and wireless communications. The suggested antenna achieves a gain of 10.05 on average. The prototyped model conformability analysis of the antenna is also performed, and good matching with simulation results is found.

1. INTRODUCTION

To establish communication on higher frequency bands in wireless communication, we need antennas of compact in nature, being conformal, low cost and should have ease in fabrication. The ongoing developments in multifunctional and high-speed devices present a promising landscape for multiband antennas characterized by their compact dimensions [1, 2]. Microstrip antennas emerge as being particularly advantageous among multiband antennas due to their compact structure and low profile. However, microstrip patch antennas suffer from notable drawbacks, including low gain, high loss, low radiation efficiency, and restricted bandwidth. To address these challenges, various approaches are being employed [3, 4]. Some of them include utilizing arrays of patch antennas [5], adjusting substrate thickness [6], incorporating multiple layers of substrates [7], and modification of the basic shape of the patch, using metamaterials and metasurface. A metasurface structure [33, 34, 36], comprising nonuniform or uniform patches with multiple unit cells [8], holds the potential to enhance radiation efficiency [9, 10] and expand operating bandwidth [11, 12, 35].

Mutual coupling has a major impact on the radiation properties in the setting of an antenna array. To lessen this coupling effect, it is imperative to maintain a separation distance between array elements ranging from $\lambda_g/2$ to λ_g, contingent upon the angular scan range [13]. Several techniques have been proposed to alleviate the coupling effect among array elements [14], including the incorporation of electromagnetic band gap structures [15], the implementation of neutralization techniques [16], and the utilization of defected ground structures. A strategic application of Characteristic Mode Analysis (CMA) proves effective in reducing coupling between array elements. Within the framework of CMA, the values of Modal Significance (MS) are calculated during antenna design within the desired operating bands [17, 18]. For instance, Li and Chen utilized Characteristic Mode Analysis to optimize the structure of the radiation element by examining surface current distributions of the metasurface and achieved three modal significances to provide dual-band characteristics [19]. In a quest to enhance antenna efficiency. Gao et al. employed CMA, investigating the surface current of the radiation element [20]. By using the Characteristic Mode Analysis approach, the antenna's bandwidth is increased, and undesired high-order resonant modes are suppressed [21, 22].

In this research, we introduce a microstrip-fed metasurface antenna designed for wireless communications. The analysis is conducted using the source-free Characteristic Mode Analysis (CMA) method, offering a profound understanding of the antenna's operational mechanisms. The metasurface is composed of a 3×3 array of nonuniform elements. We used the 3D full-wave CST Microwave Studio [37] to develop, simulate, and optimize the antenna structure. Section 2 outlines the design process of the proposed antenna, while Section 3 delves into the concept of characteristic mode analysis, with particular attention paid to metrics like modal significance, eigenvalue, and characteristic angle. Section 4 presents the conformability analysis of the proposed antenna, and Section 5 provides a comprehensive examination of various results related to the antenna design. The final section contains the concluding observations on the proposed work.

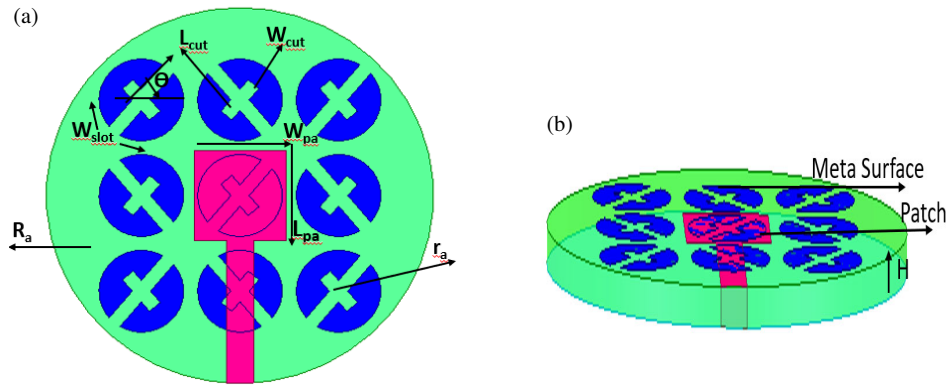* Corresponding author: Boddapati Taraka Phani Madhav (btpmadhav@kluniversity.in).

FIGURE 1. The single substrate metasurface antenna, (a) top view and (b) side view.

2. PROPOSED ANTENNA DESIGN

Both the top and side views of the envisioned design for the metasurface nonuniform array antenna are illustrated in Fig. 1. This antenna configuration encompasses a solitary substrate housing nonuniform array elements and a patch antenna integrated onto the metasurface. The substrate takes on a circular shape defined by the radius 'R_a' and a specified height 'H'. The substrate of this design is made of polyamide, which has a relative permittivity of 4.3. Copper is the conducting material used in the antenna. Interestingly, the entire bottom portion of the substrate is covered by the ground plane.

The substrate features a rectangular patch atop it, characterized by a width of 'W_{pa}' and a length of 'L_{pa}'. Ensuring 50 Ω impedance matching involves the application of a microstrip line feeding technique. The figure shows the antenna design's top view and reveals a metasurface crafted with a 3×3-unit cell array, each separated by 2 mm. Within the circular radiating element with radius 'r_a', a strategic cut is implemented, symmetrically dividing it into two partitions. One partition exhibits a slot with width 'W_{slot}', while the other section boasts a cut with a length of 'L_{cut}' and width 'W_{cut}'. This division enhances the coupling effect between the antenna and metasurface. The circular array element further introduces a rotation angle denoted as 'θ', positioned between the slot's center and the x-axis. To optimize the coupling effect, elements with a counterclockwise rotation angle are strategically positioned in all four corners, complemented by elements with a clockwise rotation angle. The dimensional specifications of the designed antenna are detailed in Table 1.

3. CHARACTERISTIC MODE ANALYSIS

The inception of the Theory of Characteristic Modes (TCMs) dates back to 1965 [23] and underwent reformulation to compute characteristic modes specifically for perfectly electric conducting bodies [24, 25]. TCM has emerged as a highly favored methodology for microstrip patch antenna design due to its capacity to offer profound insights into the radiating properties of the antenna. Interestingly, the CM theory is not dependent on the excitation; rather, it only depends on the dimensions and form of the conducting element. The modes in TCM are current modes that are closely related to eigenvalues (λ) that can be

TABLE 1. The parameters and its measurements of antenna (unit: mm).

Parameter	value
R_a circular substrate radius	27.5
H substrate thickness	2
L_{pa} patch length	13.27
W_{pa} patch width	13
r_a circle radius	6
L_{cut} cut length	2
W_{cut} cut width	2
θ angle	40 deg
W_{slot} slot width	2

calculated numerically for perfectly electric conducting bodies of any shape. There are two main processes involved in applying the characteristic mode technique to antenna design. First, the conducting elements' dimensions and shapes are optimized. An acceptable feeding position is then chosen using the current distributions that CMA has provided as guidance. In [26], characteristic modes' various uses in antenna design are explained in depth, along with their derivations. The eigenvalue equation can be solved to yield the characteristic currents.

$$X[\vec{J_n}] = \lambda_n R[\vec{J_n}] \tag{1}$$

Within this framework, the symbol λ_n represents eigenvalues, while $\vec{J_n}$ denotation indicates eigen currents or eigenfunctions. 'R' and 'X' denote the real and imaginary components of the impedance matrix, respectively, whereas the variable 'n' represents the order of the respective mode [27].

$$Z = R + JX \tag{2}$$

The eigenvalue stands out as a crucial parameter, as its magnitude holds key information regarding characteristic mode radiation and resonant frequency. Specifically, a higher magnitude of the eigenvalue, denoted as $|\lambda_n = 0|$, signifies that the mode exhibits more efficient radiation [28–31].

Characteristic Angle (CA) is a crucial element in this analysis. This angle represents the phase lag that exists on a conductor object between the surface current and the electric field [21, 32]. In terms of math, it is represented as:
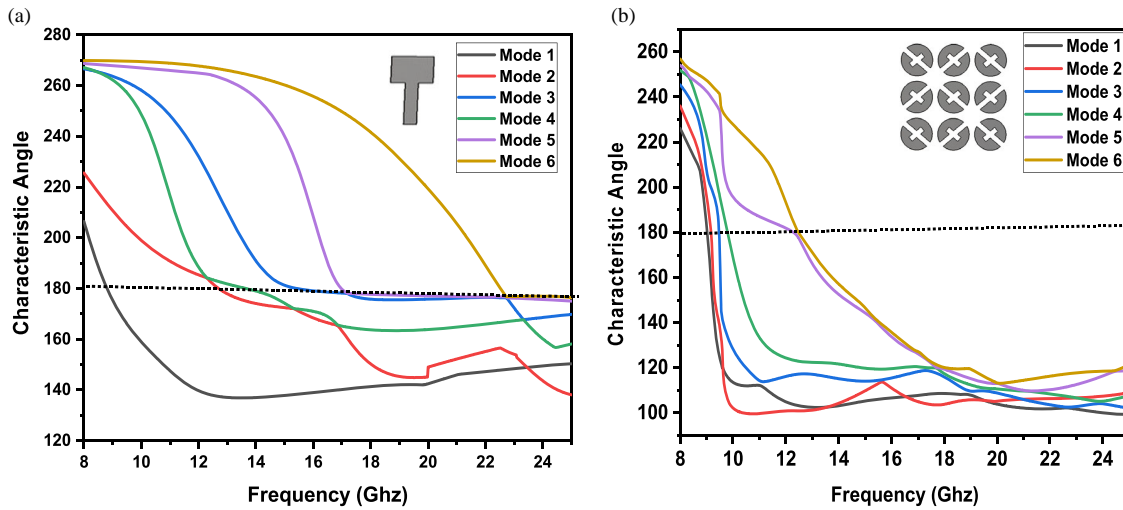
$$\alpha_n = 180 - \tan^{-1} \lambda_n \tag{3}$$

FIGURE 2. CA plot of proposed (a) patch antenna and (b) metasurface.
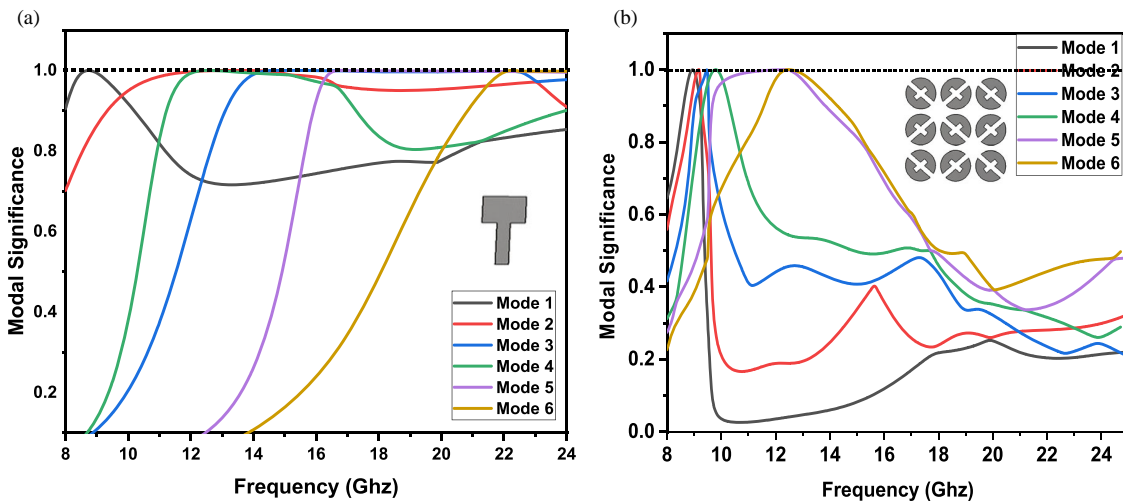

FIGURE 3. MS plot of proposed (a) patch antenna and (b) metasurface.

Modal Significance (MS) is another important element. This parameter is essential for figuring out the radiating bands and resonance frequency of a given mode. It is given a mathematical representation [29, 33].

$$\text{MS} = \frac{1}{|1 + J\lambda_n|} \quad (4)$$

When $\lambda_n = 0$, MS = 1, and $\alpha_n = 180$, a mode in CMA is said to be resonant [29]. Fig. 2(a) shows the frequency vs. characteristic angle of the patch antenna. It is clear from Fig. 2(b) that modes 1 through 6 are regarded as resonant because, at a given frequency, the characteristic angle variation for each mode achieves a 180° phase lag. The frequencies of mode 1 through mode 6 are 8.8 GHz, 12.5 GHz, 13.4 GHz, 15.3 GHz, 16.9 GHz, and 22.5 GHz. Fig. 2(b) displays the frequency vs characteristic angle of the metasurface and reveals that the resonant frequencies of 8.8 GHz, 9.1 GHz, 9.4 GHz, 9.7 GHz, 12.3 GHz, and 12.5 GHz are for modes 1, 2, 3, 4, 5, and 6.

Figure 3(a) presents the modal significance report for the suggested patch antenna design with respect to operating bands of frequency, while Fig. 3(b) presents the metasurface. These figures show that modes 1, 2, 3, 4, 5, and 6 have modal significances that are close to unity, indicating that these modes are resonant.

Figure 4(a) shows the eigenvalue analysis for the suggested patch antenna with regard to the resonant frequency, and Fig. 4(b) shows the metasurface. Figs. 4(a) and 4(b) show that modes 1 through 6 have eigenvalues that are getting close to zero, indicating that these modes are resonance frequencies throughout the frequency range.

Figure 5 shows the surface current distributions of the suggested patch antenna for each of the six modes, and Fig. 6 shows the metasurface. To obtain the necessary frequency bands, the precise feeding site is determined using the provided current distributions.
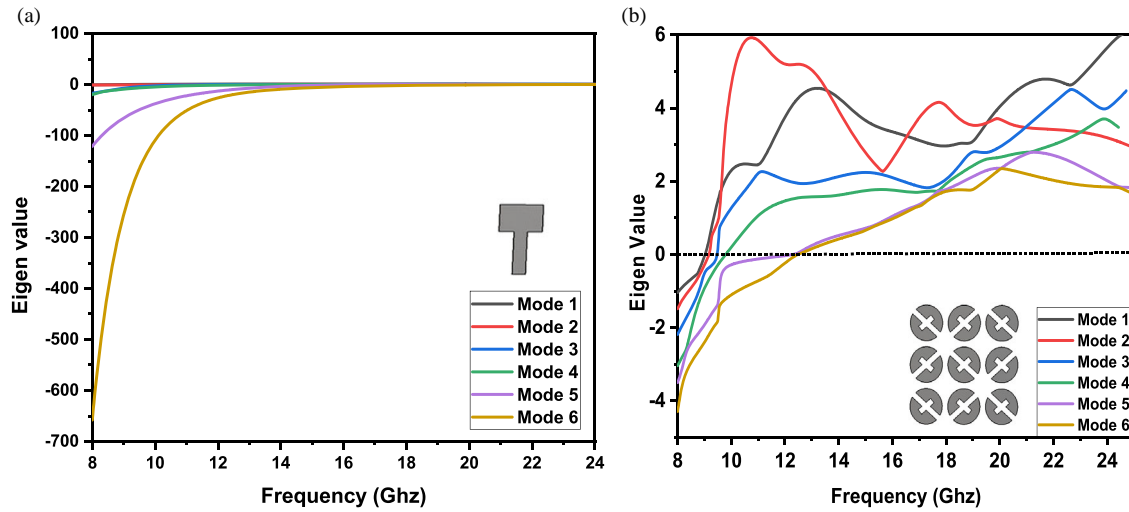
FIGURE 4. Eigen value plot of (a) proposed patch antenna and (b) metasurface.
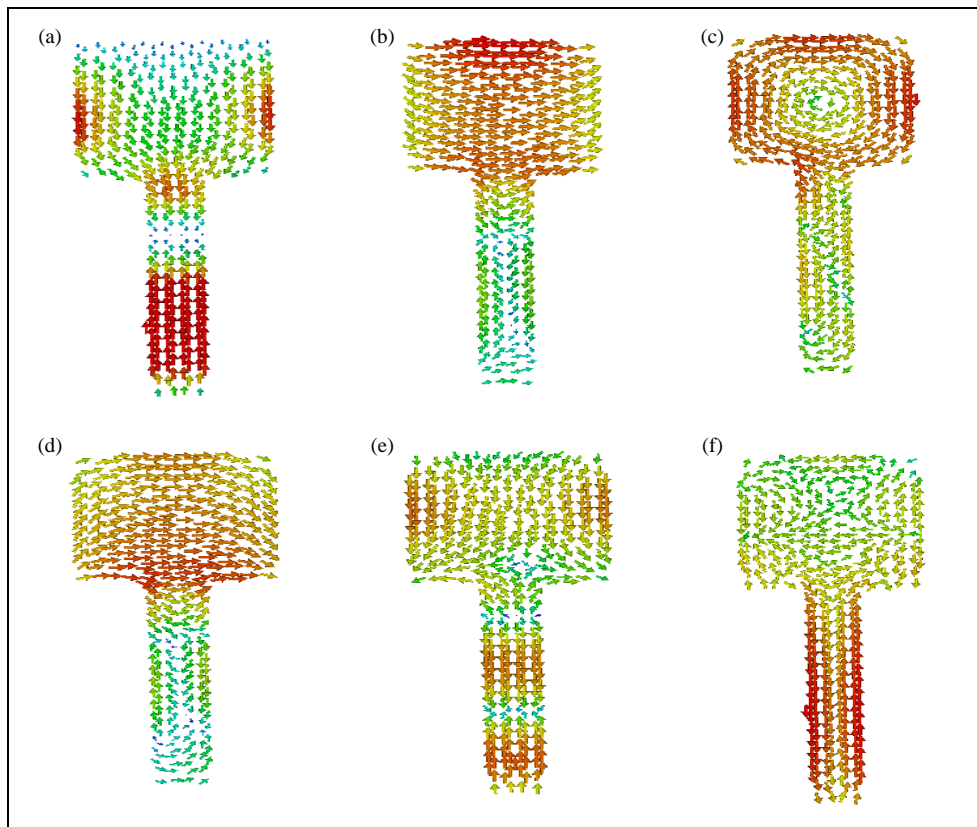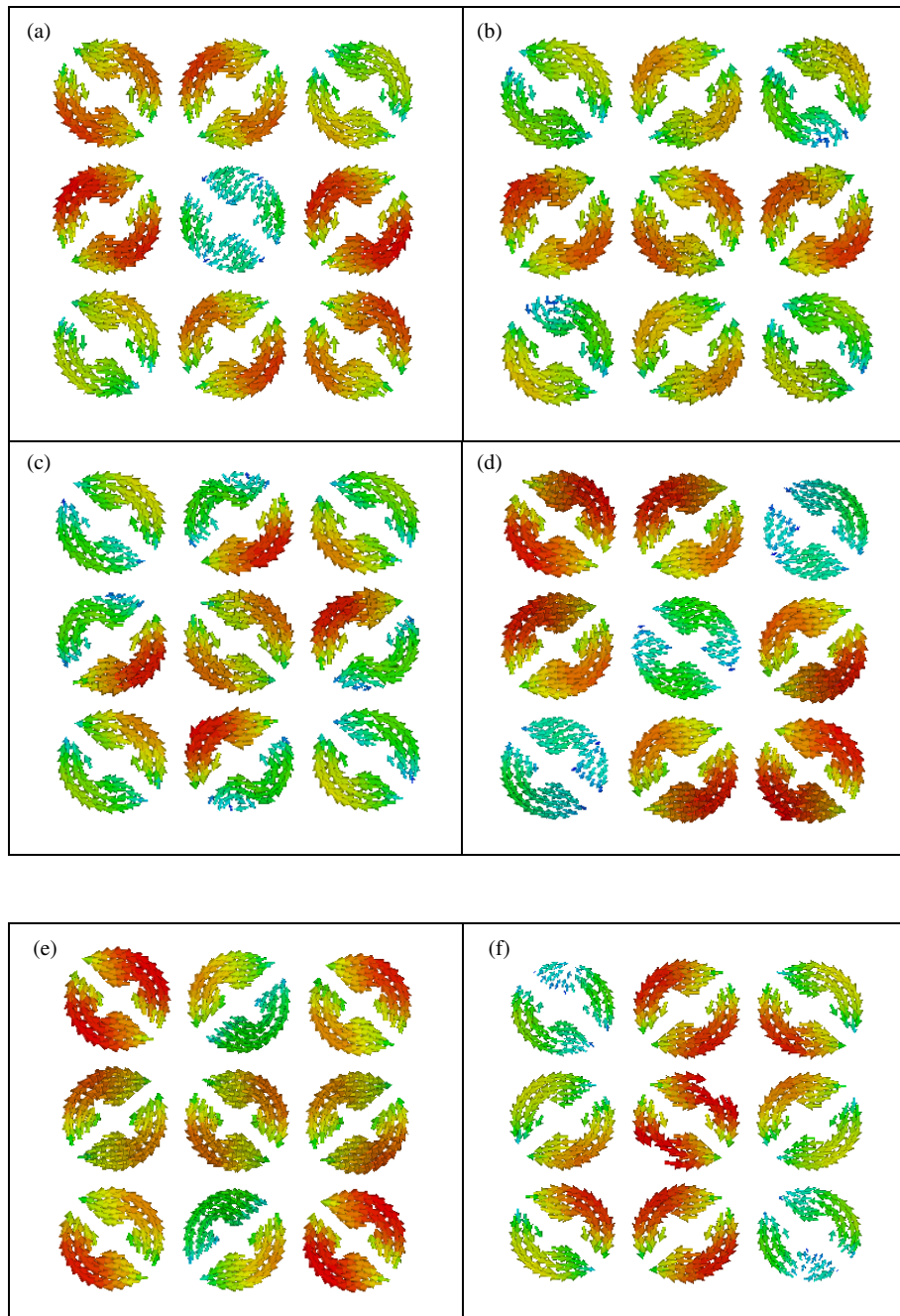

FIGURE 5. Mode 1 to mode 6 current distributions of the suggested patch antenna.

Six modes are found to resonate in relation to characteristic angle, modal significance, and eigenvalue when the suggested antenna is examined using characteristic mode analysis.

4. CONFORMABILITY ANALYSIS

Conformability emerges as a critical requirement for flexible devices, presenting a notable advantage in the proposed an-

tenna design. Ensuring consistent radiation performance in both curved and flat conditions is imperative. Conformability analysis was executed by bending the designed antenna on a cylindrical foam. The proposed antenna underwent bending at angles of 20, 30, and 60 degrees on a cylindrical form. Fig. 7 depicts the $|S_{11}|$ results for both the planar and conformal antennas, revealing nearly identical outcomes. This demonstrates the reconfigurability of the proposed antenna, rendering it suit-

FIGURE 6. Metasurface surface current distributions of (a) mode 1, (b) mode 2, (c) mode 3, (d) mode 4, (e) mode 5, (f) mode 6.

TABLE 2. Analytical comparison of the literature and the proposed antenna design.

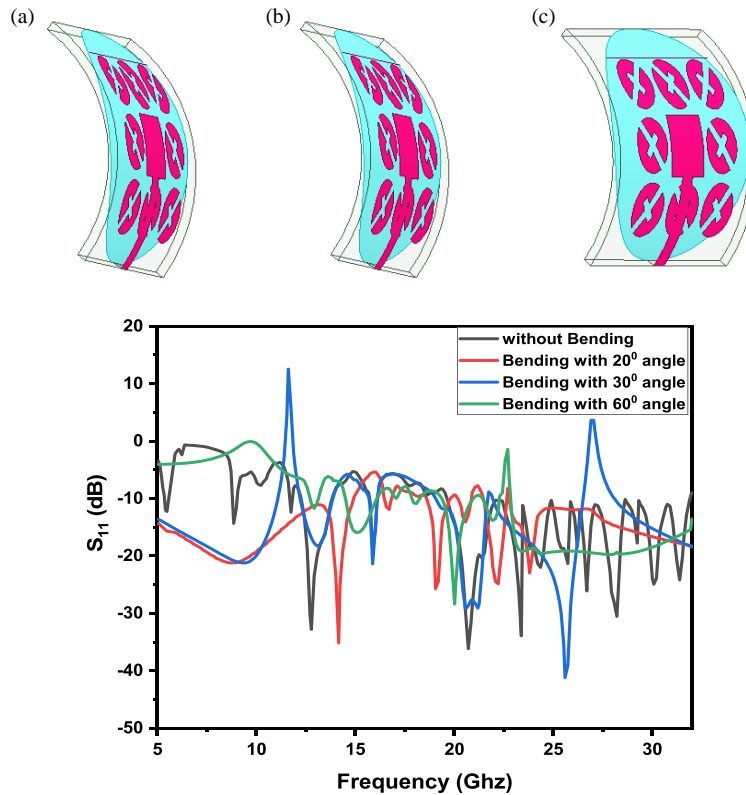| Reference	Measurements (mm × mm)	Operating Frequency (GHz)	Gain (dBi)	Efficiency
[21]	$27.5^2 \times \pi$	5.07–5.94	7.63	> 80%
[32]	$27.5^2 \times \pi$	5.5–6.1	7.9	> 90%
[35]	0.6×0.3	0.35–0.75 (THz)	5.49	> 85%
[36]	75×8	3.5, 4.9	7.67, 7.28	NR
proposed	$27.5^2 \times \pi$	5.4, 8.9, 12.8, 15.9, 19.8–31.58	10.05	84%

FIGURE 7. S_{11} of conformal antenna with an angle of 20°, 30° and 60°.
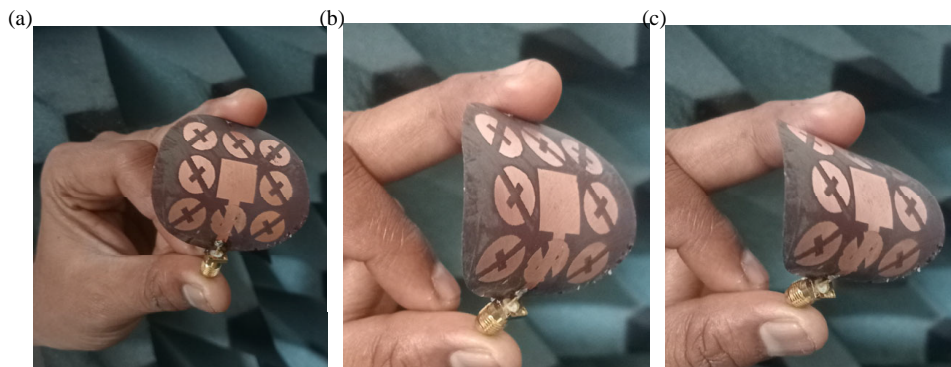

FIGURE 8. Prototyped model bending, (a) 20°, (b) 30°, (c) 60°.

able for diverse applications. Fig. 8 further illustrates images of the prototyped model undergoing bending at 20, 30, and 60-degree angles, affirming its conformable nature.

The 2D radiation patterns of the bending metasurface with an angle of 20°, 30°, and 60° are shown in Figs. 9, 10, and 11.

5. RESULTS AND DISCUSSIONS

The three-dimensional and 2D gain plots for earmarked frequencies of the proposed antenna are presented in Fig. 12. The gain plots at different resonant frequencies of various modes are analyzed and presented. At 5.4 GHz, a maximum gain of 7.53 dB is attained. At 8.8 GHz, mode 1 of both patch antenna and metasurface are resonating, attaining a maximum gain of 8.13 GHz. At 12.5 GHz, mode 2 of patch and mode 6 of metasurface are resonating, attaining a maximum gain of 9.21 dB.

The suggested antenna's computed and observed reflection coefficients are shown in Fig. 13, demonstrating their flawless agreement. The simulated and measured gains and efficiencies are shown in Fig. 14. The average gain of 10.05 dB and efficiency of 84% are achieved.

Figure 15 offers the configuration for the measurement. Table 2 tabulates the results of the analytical comparison between the suggested antenna design and the literature. Comparing the gain and bandwidth to current antenna types, the performance parameters are improved.
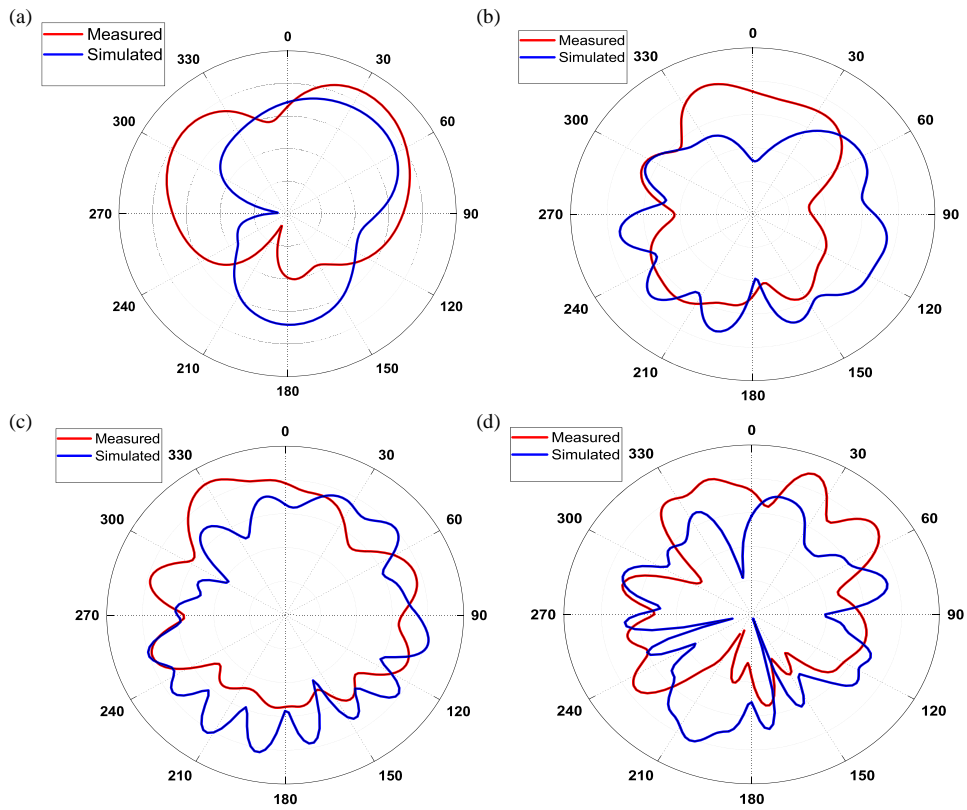
FIGURE 9. The metasurface bending with angle 20° measured vs simulated 2D radiation patterns, (a) 5.4 GHz, (b) 8.8 GHz, (c) 12.5 GHz, (d) 15.9 GHz.
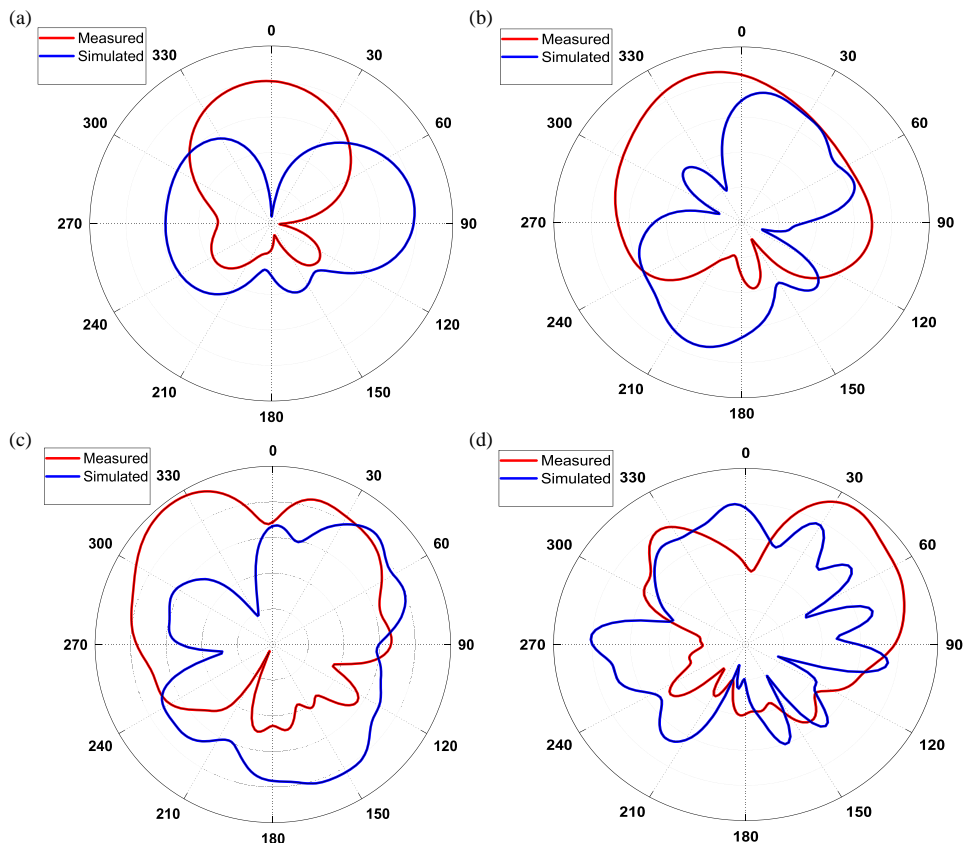
FIGURE 10. The metasurface bending with angle 30° measured vs simulated 2D radiation patterns, (a) 5.4 GHz, (b) 8.8 GHz, (c) 12.5 GHz, (d) 15.9 GHz.
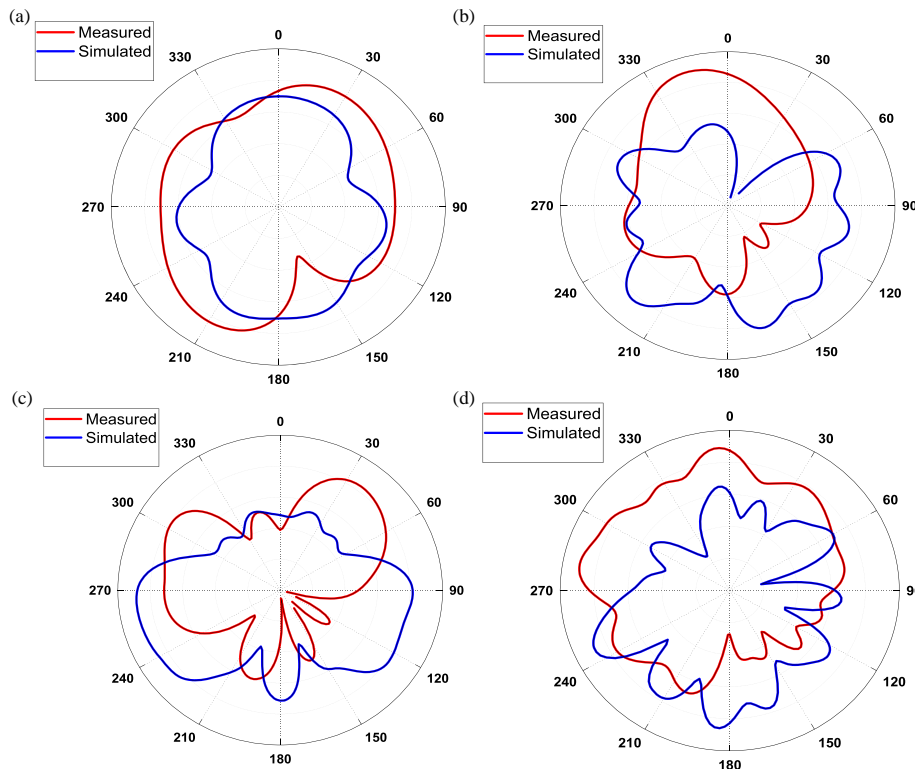
FIGURE 11. The metasurface bending with angle 60° measured vs simulated 2D radiation patterns, (a) 5.4 GHz, (b) 8.8 GHz, (c) 12.5 GHz, (d) 15.9 GHz.
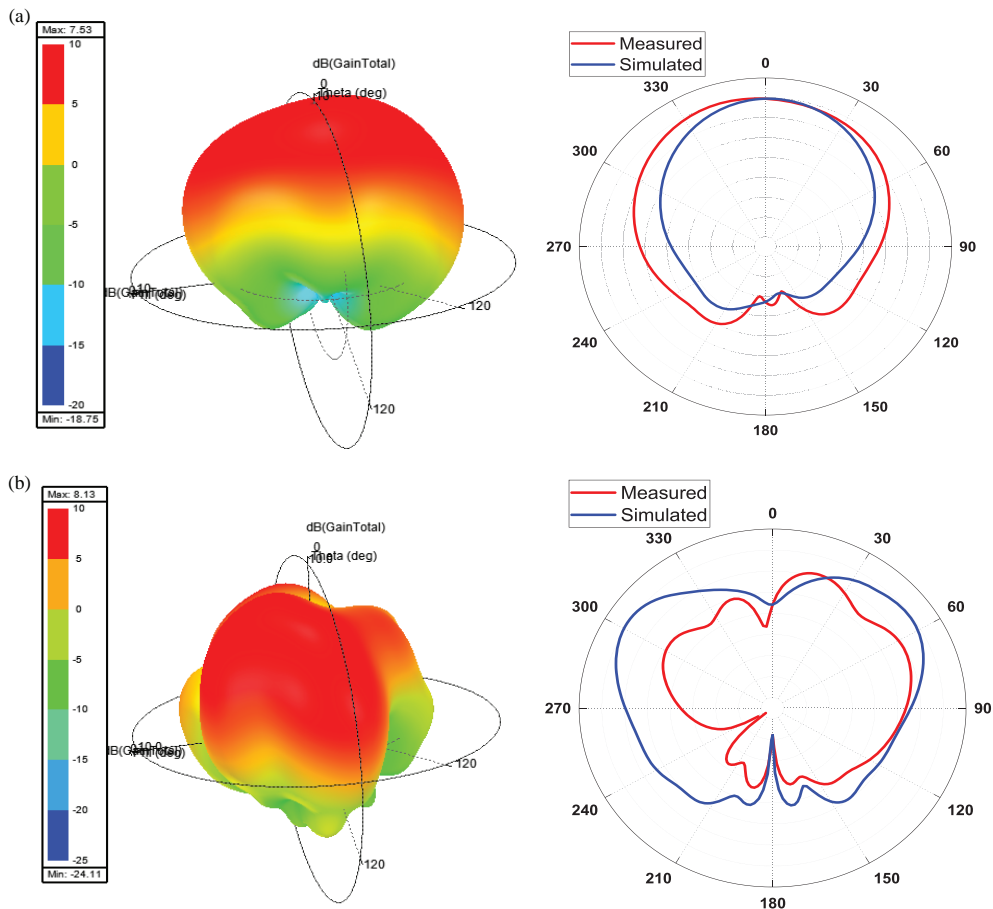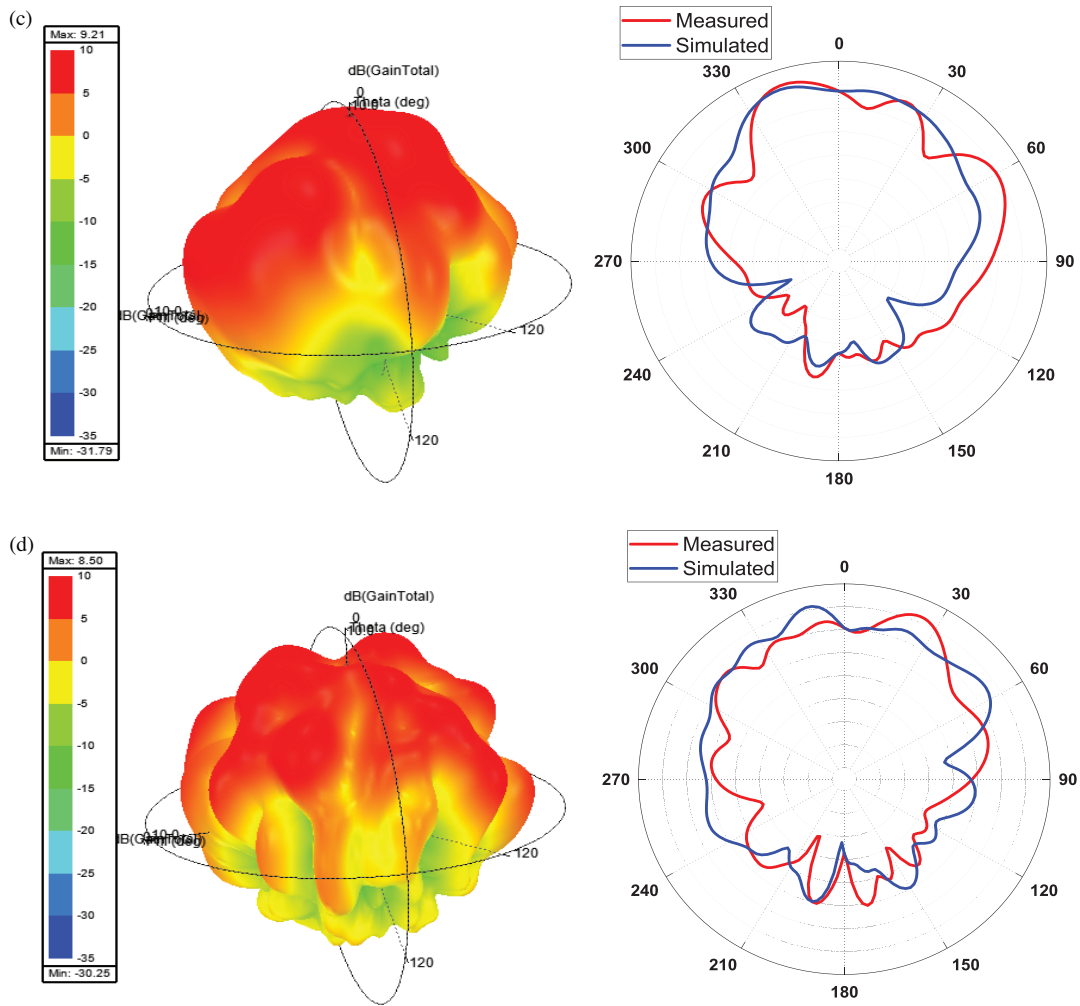
FIGURE 12. The antenna's measured vs simulated 3D and 2D radiation patterns, (a) 5.4 GHz, (b) 8.8 GHz, (c) 12.5 GHz, (d) 15.9 GHz.
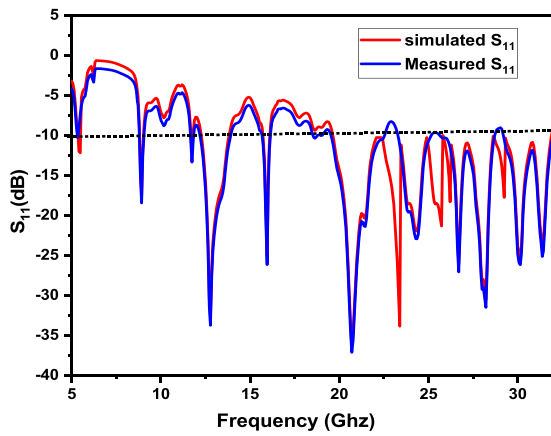

FIGURE 13. The intended antenna's S_{11} (reflection coefficient) of measurement vs simulation.
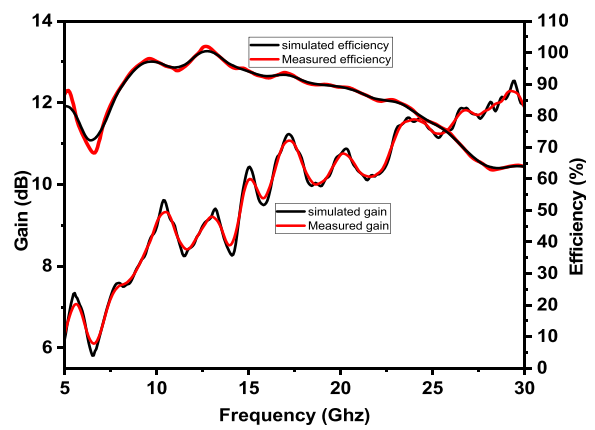
FIGURE 14. Measured and simulated suggested antenna's efficiencies and gains.

FIGURE 15. The measurement setup of antenna.

6. CONCLUSION

A multi-band microstrip fed metasurface antenna has been meticulously built and optimized in this work. Characteristic Mode Analysis (CMA) is used in the optimization process to improve the performance characteristics of the antenna. An extensive presentation of the results is provided by analyzing key factors in connection to the resonant frequency of the constructed antenna, including characteristic angle, modal significance, and eigenvalues. The distribution of surface currents for both the metasurface and patch antenna is meticulously examined and presented. To achieve the desired mode, a microstrip feed is strategically employed. The results, obtained through both measurements and simulations, reveal that the proposed antenna resonates at frequencies of 5.4 GHz, 8.9 GHz, 12.8 GHz, 15.9 GHz, and 19.8–31.58 GHz. Impressively, the antenna achieves an average gain of 10.05 dBi, an efficiency of 84%, and demonstrates agreement between modelling and test data.

ACKNOWLEDGEMENT

REFERENCES

[1] Lu, X., C. R. Chappidi, X. Wu, and K. Sengupta, "Antenna pre-processing and element-pattern shaping for multi-band mmWave arrays: Multi-port receivers and antennas," *IEEE Journal of Solid-State Circuits*, Vol. 55, No. 6, 1455–1470, Jun. 2020.

[2] Zhang, J., E. Björnson, M. Matthaiou, D. W. K. Ng, H. Yang, and D. J. Love, "Prospective multiple antenna technologies for beyond 5G," *IEEE Journal on Selected Areas in Communications*, Vol. 38, No. 8, 1637–1660, Aug. 2020.

[3] Kumar, A., R. Khandelwal, S. Singh, A. Kumar, and A. Makhdumi, "A review on gain enhancement techniques of microstrip antenna," in *2021 2nd International Conference on Intelligent Engineering and Management (ICIEM)*, IEEE, 2021.

[4] Kumar, A., N. Gupta, and P. C. Gautam, "Gain and bandwidth enhancement techniques in microstrip patch antennas — A review," *International Journal of Computer Applications*, Vol. 148, No. 7, 9–14, 2016.

[5] Islam, M. A. and N. C. Karmakar, "A 4 × 4 dual polarized mm-Wave ACMPA array for a universal mm-Wave chipless RFID tag reader," *IEEE Transactions on Antennas and Propagation*, Vol. 63, No. 4, 1633–1640, 2015.

[6] Kovitz, J. M. and Y. Rahmat-Samii, "Using thick substrates and capacitive probe compensation to enhance the bandwidth of traditional CP patch antennas," *IEEE Transactions on Antennas and Propagation*, Vol. 62, No. 10, 4970–4979, Oct. 2014.

[7] Zhang, C., X.-Y. Cao, J. Gao, and S.-J. Li, "Wideband high-gain and low scattering antenna using shared-aperture metamaterial superstrate," *Radioengineering*, Vol. 27, No. 2, 379–385, Jun. 2018.

[8] Li, H.-P., G.-M. Wang, X.-J. Gao, J.-G. Liang, and H.-S. Hou, "An X/Ku-band focusing anisotropic metasurface for low cross-polarization lens antenna application," *Progress In Electromagnetics Research*, Vol. 159, 79–91, 2017.

[9] Minatti, G., E. Martini, and S. Maci, "Efficiency of metasurface antennas," *IEEE Transactions on Antennas and Propagation*, Vol. 65, No. 4, 1532–1541, Apr. 2017.

[10] Lin, F. H. and Z. N. Chen, "A method of suppressing higher order modes for improving radiation performance of metasurface multiport antennas using characteristic mode analysis," *IEEE Transactions on Antennas and Propagation*, Vol. 66, No. 4, 1894–1902, Apr. 2018.

[11] Liu, S., D. Yang, Y. Chen, K. Sun, X. Zhang, and Y. Xiang, "Design of single-layer broadband omnidirectional metasurface antenna under single mode resonance," *IEEE Transactions on Antennas and Propagation*, Vol. 69, No. 10, 6947–6952, Oct. 2021.

[12] Li, H.-P., G.-M. Wang, J.-G. Liang, and X.-J. Gao, "Wideband multifunctional metasurface for polarization conversion and gain enhancement," *Progress In Electromagnetics Research*, Vol. 155, 115–125, 2016.

[13] Balanis, C. A., *Antenna Theory: Analysis and Design*, John Wiley & Sons, 2016.

[14] Lui, H. S. A. and T. S. Bird, "Techniques for minimizing mutual coupling effects in arrays," *Mutual Coupling Between Antennas*, 325–356, 2021.

[15] Iluz, Z., R. Shavit, and R. Bauer, "Microstrip antenna phased array with electromagnetic bandgap substrate," *IEEE Transactions on Antennas and Propagation*, Vol. 52, No. 6, 1446–1453, 2004.

[16] Diallo, A., C. Luxey, P. L. Thuc, R. Staraj, and G. Kossiavas, "Enhanced two-antenna structures for universal mobile telecommunications system diversity terminals," *IET Microwaves, Antennas & Propagation*, Vol. 2, No. 1, 93–101, 2008.

[17] Li, T. and Z. N. Chen, "Metasurface-based shared-aperture 5G S-/K-band antenna using characteristic mode analysis," *IEEE Transactions on Antennas and Propagation*, Vol. 66, No. 12, 6742–6750, 2018.

[18] Liu, S., D. Yang, and J. Pan, "A low-profile broadband dual-circularly-polarized metasurface antenna," *IEEE Antennas and Wireless Propagation Letters*, Vol. 18, No. 7, 1395–1399, 2019.

[19] Li, T. and Z. N. Chen, "A dual-band metasurface antenna using characteristic mode analysis," *IEEE Transactions on Antennas and Propagation*, Vol. 66, No. 10, 5620–5624, 2018.

[20] Gao, X., G. Tian, Z. Shou, and S. Li, "A low-profile broadband circularly polarized patch antenna based on characteristic mode analysis," *IEEE Antennas and Wireless Propagation Letters*, Vol. 20, No. 2, 214–218, 2021.

[21] Gao, G., R.-F. Zhang, W.-F. Geng, H.-J. Meng, and B. Hu, "Characteristic mode analysis of a nonuniform metasurface antenna for wearable applications," *IEEE Antennas and Wireless Propagation Letters*, Vol. 19, No. 8, 1355–1359, 2020.

[22] Wang, K., W. Shao, X. Ding, B.-Z. Wang, and B. Jiang, "Design of high-gain metasurface antenna based on characteristic mode analysis," *IEEE Antennas and Wireless Propagation Letters*, Vol. 21, No. 4, 661–665, 2022.

[23] Falcone, F., T. Lopetegi, M. A. G. Laso, J. D. Baena, J. Bonache, M. Beruete, R. Marqués, F. Martín, and M. Sorolla, "Babinet principle applied to the design of metasurfaces and metamaterials," *Physical Review Letters*, Vol. 93, No. 19, 197401, 2004.

[24] Garbacz, R. J., "Modal expansions for resonance scattering phenomena," *Proceedings of the IEEE*, Vol. 53, No. 8, 856–864, 1965.

[25] Harrington, R. and J. Mautz, "Theory of characteristic modes for conducting bodies," *IEEE Transactions on Antennas and Propagation*, Vol. 19, No. 5, 622–628, 1971.

[26] Harrington, R. and J. Mautz, "Computation of characteristic modes for conducting bodies," *IEEE Transactions on Antennas and Propagation*, Vol. 19, No. 5, 629–639, Sep. 1971.

[27] Chen, Y. and C.-F. Wang, *Characteristic Modes: Theory and Applications in Antenna Engineering*, John Wiley & Sons, 2015.

[28] Gao, X., G. Tian, Z. Shou, and S. Li, "A low-profile broadband circularly polarized patch antenna based on characteristic mode analysis," *IEEE Antennas and Wireless Propagation Letters*, Vol. 20, No. 2, 214–218, 2021.

[29] Adams, J. J., S. Genovesi, B. Yang, and E. Antonino-Daviu, "Antenna element design using characteristic mode analysis: Insights and research directions," *IEEE Antennas and Propagation Magazine*, Vol. 64, No. 2, 32–40, 2022.

[30] Kollipara, V. and S. Peddakrishna, "Circularly polarized antennas using characteristic mode analysis: A review," *Advances in Technology Innovation*, Vol. 7, No. 4, 242–257, 2022.

[31] Hamad, E. K. I. and A. Abdelaziz, "Metamaterial superstrate microstrip patch antenna for 5G wireless communication based on the theory of characteristic modes," *Journal of Electrical Engineering*, Vol. 70, No. 3, 187–197, 2019.

[32] Bhavani, K. D., B. T. P. Madhav, S. Das, N. Hussain, S. S. Ali, and K. V. Babu, "Development of metamaterial inspired non-uniform circular array superstate antenna using characteristic mode analysis," *Electronics*, Vol. 11, No. 16, 2517, 2022.

[33] Pan, Y. M., P. F. Hu, X. Y. Zhang, and S. Y. Zheng, "A low-profile high-gain and wideband filtering antenna with metasurface," *IEEE Transactions on Antennas and Propagation*, Vol. 64, No. 5, 2010–2016, 2016.

[34] Nasimuddin, , X. Qing, and Z. N. Chen, "Metasurface-based low profile broadband circularly polarized antenna," in *Proceedings of TENCON 2017 — 2017 IEEE Region 10 Conference*, 2378–2382, Penang, Malaysia, 2017.

[35] Babu, K. V., S. Das, G. N. J. Sree, B. T. P. Madhav, S. K. K. Patel, and J. Parmar, "Design and optimization of micro-sized wideband fractal MIMO antenna based on characteristic analysis of graphene for terahertz applications," *Optical and Quantum Electronics*, Vol. 54, No. 5, 281, 2022.

[36] Zhuang, H., H. Tan, C. Liu, F. Li, W. Ding, C. Tian, and F. Kong, "Dual-band metasurface antenna based on characteristic mode analysis," *Progress In Electromagnetics Research M*, Vol. 117, 71–81, 2023.

[37] CST Studio Suite, "CST Microwave Studio," 2017, http://www.cst.com.